

Article

Effect of Mn Addition on Hot-Working Behavior and Microstructure of Hot-Rolled Medium-Mn Steels

Adam Skowronek ¹, Dariusz Woźniak ² and Adam Grajcar ^{1,*}

¹ Department of Engineering Materials and Biomaterials, Faculty of Mechanical Engineering, Silesian University of Technology, 18A Konarskiego Street, 44-100 Gliwice, Poland; adam.skowronek@polsl.pl

² Łukasiewicz Research Network—Institute for Ferrous Metallurgy, 12-14 K. Miarki Street, 44-100 Gliwice, Poland; dwozniak@imz.pl

* Correspondence: adam.grajcar@polsl.pl; Tel.: +48-32-237-2933

Abstract: Hot plastic working behavior and microstructure evolution were investigated during a production process of four medium-Mn steels, which differed in Mn (3 and 5%) and Nb contents. The production process started with casting, followed by hot forging, rough hot-rolling and concluded with final thermomechanical processing, which was performed to obtain multiphase bainite-based alloys with some fractions of retained austenite. The rough rolling was composed of four passes with total true strain of 0.99 and finishing rolling temperature of 850 °C, whereas thermomechanical processing contained five passes and total true strain of 0.95 at a finishing rolling temperature of 750 °C. During the process, the force parameters were recorded, which showed that the rolling forces for steels containing 3% Mn are higher compared to the 5% Mn alloys. There was no significant influence of Nb on the rolling parameters. The produced as-cast microstructures were composed of dendritic bainitic-martensitic phases. A positive effect of Nb micro-addition on a refinement of the as-cast structure was noticed. The thermomechanical processed steels showed fine multiphase microstructures with some fractions of retained austenite, the fraction of which depended on the Mn content in steel. The steels containing 3% Mn generated higher forces both during rough and thermomechanical rolling, which is related to slower recrystallization softening in these alloys compared to the steels containing 5% Mn.

Keywords: advanced high-strength steel; hot-rolling; bainitic steel; manganese addition; semi-industrial simulation; microalloying



Citation: Skowronek, A.; Woźniak, D.; Grajcar, A. Effect of Mn Addition on Hot-Working Behavior and Microstructure of Hot-Rolled Medium-Mn Steels. *Metals* **2021**, *11*, 354. <https://doi.org/10.3390/met11020354>

Academic Editor: Denis Jorge-Badiola

Received: 22 January 2021

Accepted: 16 February 2021

Published: 19 February 2021

Publisher's Note: MDPI stays neutral with regard to jurisdictional claims in published maps and institutional affiliations.



Copyright: © 2021 by the authors. Licensee MDPI, Basel, Switzerland. This article is an open access article distributed under the terms and conditions of the Creative Commons Attribution (CC BY) license (<https://creativecommons.org/licenses/by/4.0/>).

1. Introduction

The modern automotive industry uses mainly AHSS (Advanced High Strength Steels) steels for car body constructions [1,2]. These are multiphase steels which, due to their complex microstructure and the use of various strengthening mechanisms, allow for obtaining increased strength while maintaining the desired plasticity. Thus, these constantly break the “banana curve” tendencies for automotive steel [3]. AHSS steels are divided into three generations: the first generation consists of low-alloy multi-phase steels, such as TRIP (Transformation Induced Plasticity), DP (dual phase) etc. [4,5] They guarantee good properties at a relatively low price of the material and its production. The second generation of AHSS significantly increased the proportion of manganese (>20%) leading to a material with unusual properties (elongation up to 80%) [6,7]. However, the disadvantages determining their negligible use turned out to be very high costs and difficulties in production.

The MMn (medium-Mn) steels belong to the third generation of AHSS (Advanced High Strength Steels) [8,9] and are currently widely developed worldwide due to their uncommon mechanical and technological properties [10,11]. These steels represent the next step in the evolution of conventional TRIP-aided (Transformation Induced Plasticity) multiphase steels. The increased manganese content (3–12%) causes the possibility of obtaining

high portion of retained austenite (up to 40%) in heat treatment or thermomechanical processes [5,12] and/or intercritical annealing [13]. The remaining phases occurring in these steels are bainite, ferrite and martensite. MMn steels show intermediate properties between the steels of generations I and II. However, intense research brings them closer to generation II in terms of mechanical properties.

MMn steels are at a relatively early stage of development. Therefore, a major part of all research is focused on heat treatment parameters' optimizations [13], studies of its various variants [14,15], and explaining the complex mechanisms occurring in these steels [16–18]. Many studies on these steels are the result of testing the material from the beginning (melting and casting) to the end (heat treatment and property testing) conducted on a laboratory scale [16,19]. This type of research is very efficient in terms of the abovementioned investigations, but the results usually differ from those obtained during final industrial production processes.

Furthermore, the first part of producing AHSS, and especially MMn steels (casting and hot rolling), is usually omitted in terms of deeper analysis in favor of the heat treatment of the material. Up-to-date hot-working behavior was investigated using dilatometry [20] or different simulators of metallurgical processes and hot deformation [21,22]. Typical techniques that are useful for the identification of hot-working response included double-hit compression [23,24] and multi-step hot torsion or hot compression tests [25]. However, there are no data from a full industrial rolling mills, and only few works concerning semi-industrial processes are available [26,27]. The future implementation of the third generation AHSSs in industrial production requires prior analysis of this approach. It is known that, with an increase in the number of alloying elements (present in second and third AHSS generations), hot-working resistance becomes higher when compared to the conventional automotive steel sheets, while manganese additionally strengthens the alloy, increasing its deformation resistance [28]. The problem is even more complex when Mn is added, together with other alloying additions typical for AHSSs, i.e., Al, Si, etc. [16,23].

Due to the shortage of data from the semi-industrial producing process of MMn steels, a detailed analysis concerning the force parameters of the hot rolling and microstructure evolution of MMn steels with the use of semi-industrial equipment was conducted. These results provide a broader view of the behavior of MMn steels under conditions similar to industrial production, which may facilitate the adaptation of rolling lines to their production, and design pilot tests on such lines. This is a necessary step in bringing any new material to the market.

2. Materials and Methods

The chemical compositions of studied steels are presented in Table 1. The alloys differ mainly in Mn content and the addition of Nb (Nb-microalloyed or Nb-free alloys). The following production steps were performed using the equipment supplied by the Łukasiewicz Research Network—Institute for Ferrous Metallurgy, Gliwice, Poland. The ingots were produced in a VIM LAB 30-75 (Seco/Warwick, Swiebodzin, Poland) vacuum furnace. The melted metal was cast at 1545 °C in an argon atmosphere into a hot-topped closed-bottom mold with dimensions bottom— \varnothing 122 mm, top— \varnothing 145 mm, height—200 mm.

Table 1. Chemical compositions of investigated alloys.

Steel	Chemical Element, wt. %								Total, wt. %
	C	Mn	Al	Si	Mo	Nb	S	P	
3Mn	0.17	3.3	1.7	0.22	0.23	-	0.014	0.010	5.4
3MnNb	0.17	3.1	1.6	0.22	0.22	0.04	0.005	0.008	5.2
5Mn	0.16	4.7	1.6	0.20	0.20	-	0.004	0.008	6.7
5MnNb	0.17	5.0	1.5	0.21	0.20	0.03	0.005	0.008	6.9

The 25 kg ingots were next austenitized at 1200 °C for 180 min and forged in a temperature range from 1200 to 900 °C to a final width of 155 mm and a thickness of 23 mm (Table 2). The different lengths of the material result from the operation of mechanically trimming the edges of the forged material and cutting off the fragments for other tests.

Table 2. Dimensions of the test samples before rough rolling.

Steel	Dimensions, mm		
	Thickness	Length	Width
3Mn	23	320	155
3MnNb		360	
5Mn		400	
5MnNb		470	

The materials' hot rolling was performed according to a scheme presented in Figure 1. The rolling trials were conducted in the semi-industrial line (Figure 2), the detailed characteristics of which are described in [29]. Both rough rolling and thermomechanical processing were preceded by the austenitization of the material in an electric resistance reheating furnace at 1200 °C for 25 and 12 min, respectively. For the rolling, the D550 two-high reversing hot-rolling mill with a roll diameter of 550 mm and a roll-barrel length of 700 mm was used. Rough rolling of test samples with a thickness of 23 mm was conducted in 4 passes in a temperature range between 1100 and 900 °C. The applied true strains were 0.20, 0.28, 0.28 and 0.24, respectively, and the final thickness of the material was ~8.5 mm. For the thermomechanical treatment process, 5 passes between 1100 and 750 °C, with true strains of 0.2, 0.2, 0.2, 0.2, and 0.14 for the final pass, were applied with a final sheet thickness of ~3.4 mm. Before and after a rolling stand, the temperature was determined automatically using pyrometers as permanent line units. In addition, the final rolling temperature was measured using a Raytek—Raynger 3i1M (Raytek GmbH, Berlin, Germany) portable pyrometer. In between the passes, material was placed between roller tables, with isothermal heating panels, which were adjusted at 500 °C to delay cooling (Figure 2). Time from the reheating furnace to the first pass was equal to 20 s and the time between successive passes was about 10 s. After rough rolling, the material was air cooled. The cooling after hot rolling in thermomechanical treatment routes was performed using air-blow and water-spray cooling devices with an isothermal step applied at 400 °C for 300 s (in electric resistance furnace for heat treatment). This cooling strategy was designed to produce the bainitic-austenitic microstructures required in advanced multiphase steels. Subsequently, the material was air cooled to room temperature.

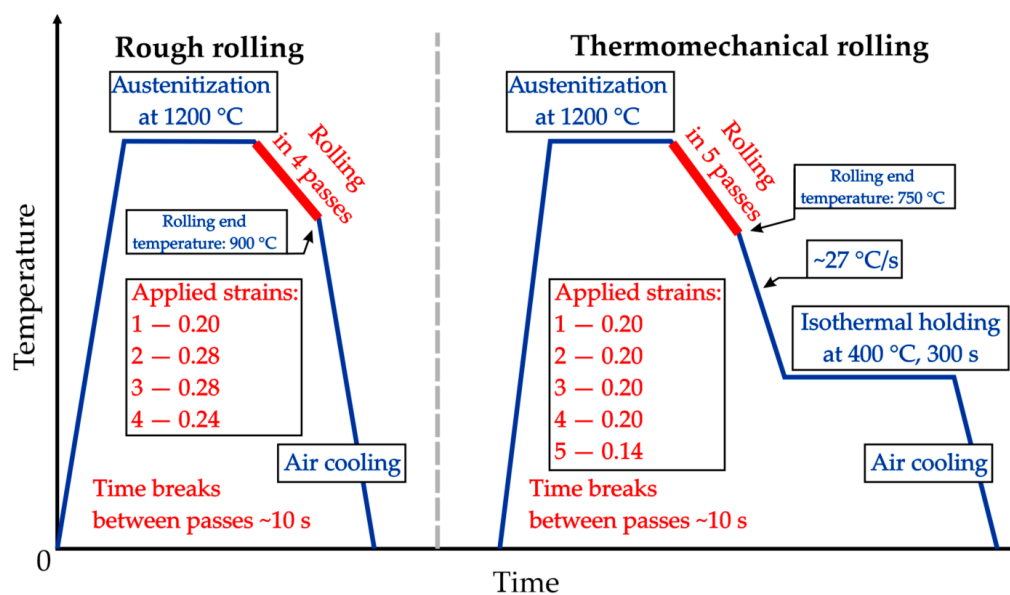


Figure 1. Schematic of materials' hot rolling processes.

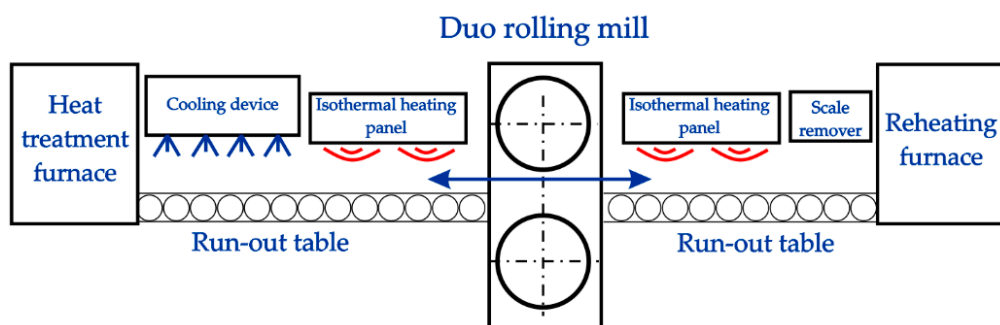


Figure 2. Schematic of the used semi-industrial line.

The crucial parameters recorded during rolling were:

- Thickness of strip;
- Rolling speed;
- Temperature of strip during cooling;
- Roll load force during rolling;
- Time of pass;
- Time between passes.

A method of measuring the load on rolls is as follows: under the lower roller bearing housings, there were hydraulic cylinders of the lower positioning of rolls equipped with safety blocks. The block consisted of a mounting plate attached to the stand housing. Proportional control distributors with an integrated electronic board and measuring connections were installed on the plate. The pressure force of the lower roll was measured by a pressure transducers on both sides of the cylinder. The pressure transducers were built into the cylinder protection blocks directly on the cylinder. Data from the transmitter in an analog form (4 to 20 mA) were transmitted to the controller. The calibration was 4 mA = 0 MPa, 20 mA = 20 MPa. The measured values were recorded on the hard disk of the rolling mill computer every 2 ms.

In order to determine the microstructure in the subsequent production steps (casting, forging, and rolling) samples of the material were grinded, polished, and etched according to standard procedures using grinding papers 220, 800, 1200, and polishing using 9, 3 and, 1 μm diamond suspensions. The as-cast and forged materials were etched in 10% aqueous solution of sodium metabisulfite for better identification of retained austenite. Nital was

used for etching as-rolled specimens. Metallographic investigations were performed using LEICA MEF4A (Leica Microsystems, Wetzlar, Germany) light microscope and Zeiss SUPRA 35 (Carl Zeiss AG, Oberkochen, Germany) scanning electron microscope.

3. Results and Discussion

3.1. Casting and Forging

Figure 3 presents images of microstructures obtained after casting (C). Due to the similarity of as-cast microstructures of 3Mn and 5Mn steels, images show representative microstructures of 5Mn and 5MnNb alloys. The microstructure of 5Mn steel after casting is characterized by dendritic morphology, which is visible in Figure 3a. The main axes of dendrites are parallel to the axis of the ingot. The Nb addition caused a positive structure refinement of the dendrites; therefore, they are less visible (Figure 3b). In both cases, the austenite decomposition products started to grow at prior austenite grain boundaries (Figure 3c,d). The prior austenite grains are relatively large. Due to high hardenability of alloys with the increased Mn content [15], the microstructures after casting are composed of martensitic-bainitic laths. Each prior austenite grain consists of a few bainitic-martensitic colonies.

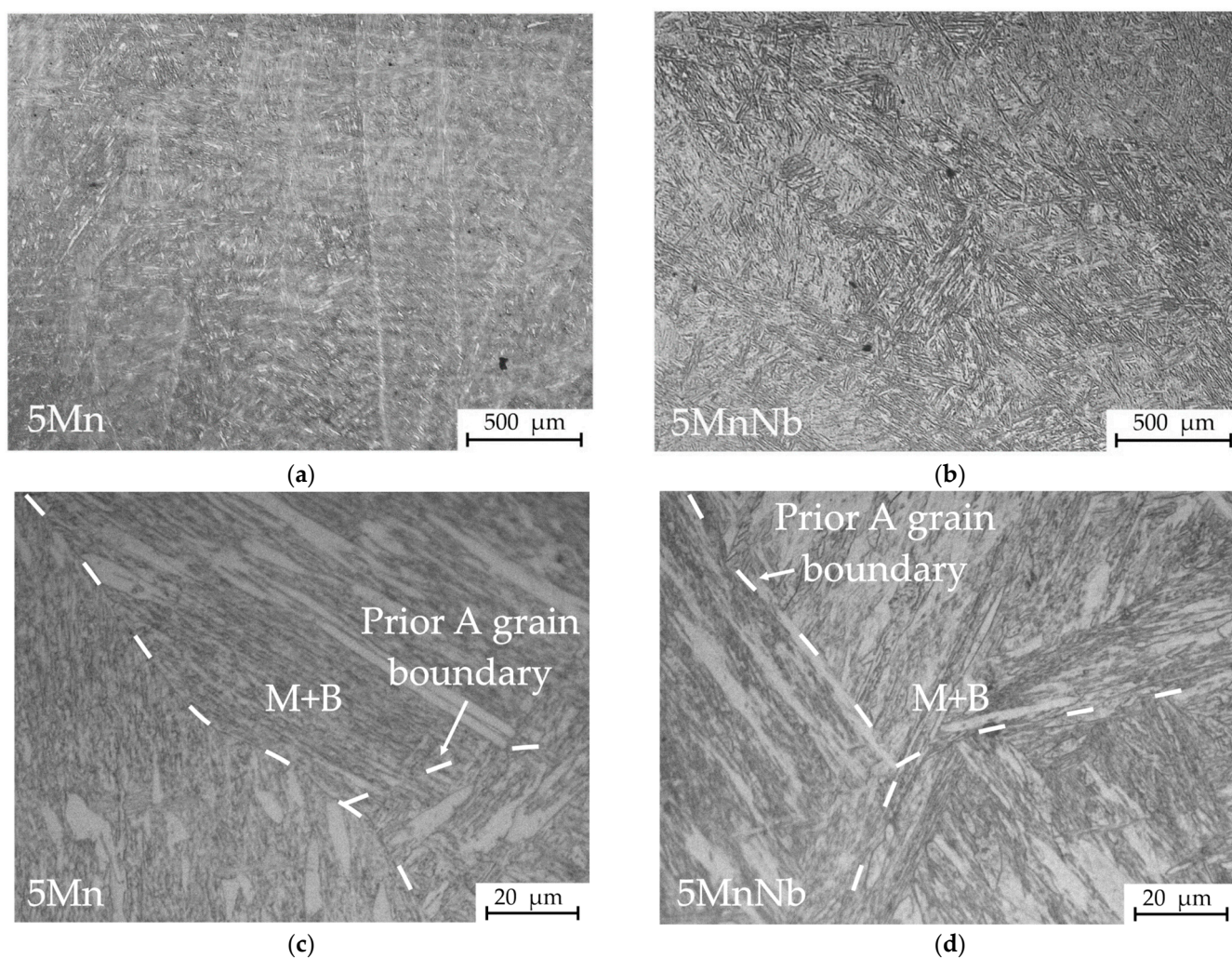


Figure 3. Microscopic images of as-cast (C) microstructures: (a) 5Mn at 50× magnification; (b) 5MnNb at 50× magnification; (c) 5Mn at 1000× magnification; (d) 5MnNb at 1000× magnification; A—prior austenite grain; M—martensite; B—bainite.

After hot forging (F), the dendritic structure disappeared (Figure 4), but the steels preserve the lath morphology. The structures are heavily refined and homogeneous, which indicates that the austenitizing of the ingots at 1200 °C for 3 h followed by hot forging

is sufficient to remove some segregations of as-cast specimens. In the case of 3Mn steels (Figure 4a,b), some fractions of retained austenite (RA) are visible in two main localizations: at the prior austenite boundaries and between the laths of martensite/bainite. The phase is characterized by very fine grains. In the case of 5Mn steels (Figure 4c,d) the retained austenite is not visible. There is a slight effect of niobium addition on the microstructure refinement of forged steels.

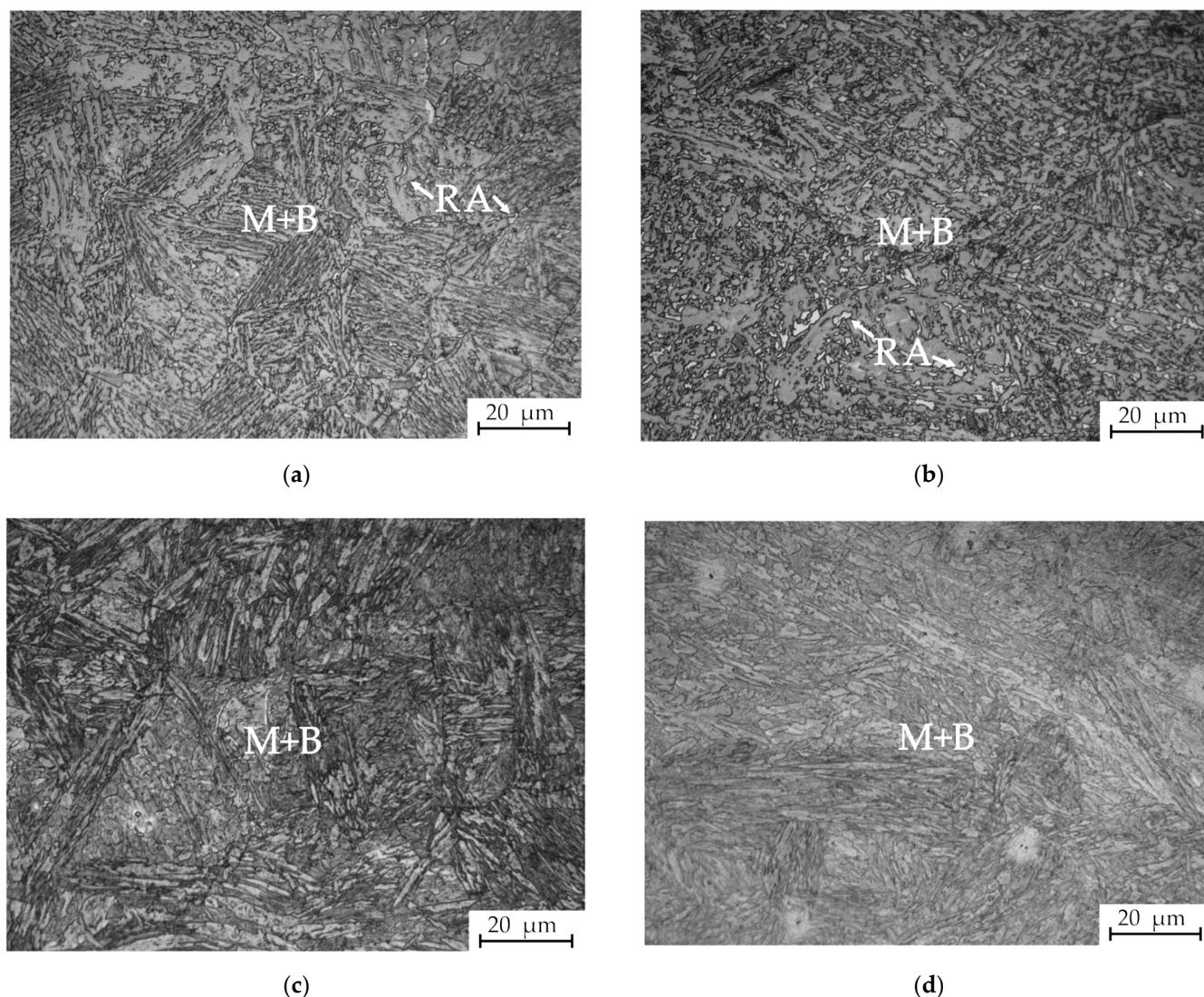


Figure 4. Microscopic images of hot-forged (F) microstructures: (a) 3Mn; (b) 3MnNb; (c) 5Mn; (d) 5MnNb; M—Martensite; B—Bainite; RA—Retained austenite.

3.2. Rough Rolling

The initial dimensions of steels subjected to rough rolling are summarized in Table 3. Figure 5a contains strain values obtained during hot rolling. The strain values coincide with the designed schedules. Figure 5b shows temperature changes in the four passes. The temperature for all steels varied in a very similar way. Samples left the reheating furnace at 1200 °C. Up to completing the first pass, the temperature decreased to about 1050 °C. The temperature decreased further and was about 900–910 after the fourth pass. These results are in line with the designed values. Figure 6a shows the roll's load change during rolling. Each vertical fragment of the diagram represents one pass and lasts ca. 2 s. The times between following passes were deleted on the diagram for better data readability but they were 10 ± 1 s each. It is visible that, during the first pass, all steels generated similar

forces. What is more interesting is that, during the next passes, the roll's loads are higher in the case of steels containing 3% of manganese. The difference increases in the following passes. It can be explained by the different hot-working behavior of the alloys containing 3 and 5% Mn. On the one hand in our earlier research, we found that the deformation resistance of the steels during hot compression is very similar, which was registered by continuous hot compression tests [30]. This explains the similar hot-deformation response of all alloys during the first pass. On the other hand, Grajcar and Kuziak [23] revealed, during double-hit compression tests, that austenite softening, expressed by a process of static recrystallization between deformation steps, is smaller in the alloys containing the 3% Mn, whereas the static recrystallization is favored in the 5Mn alloys. Therefore, the 3Mn and 3MnNb generated higher roll loads compared to the easier recrystallized 5Mn alloys.

Table 3. Dimensions of the sheet samples before thermomechanical rolling.

Steel	Dimensions, mm		
	Thickness	Length	Width
3Mn	8.5	485	170
3MnNb		500	
5Mn		580	
5MnNb		635	

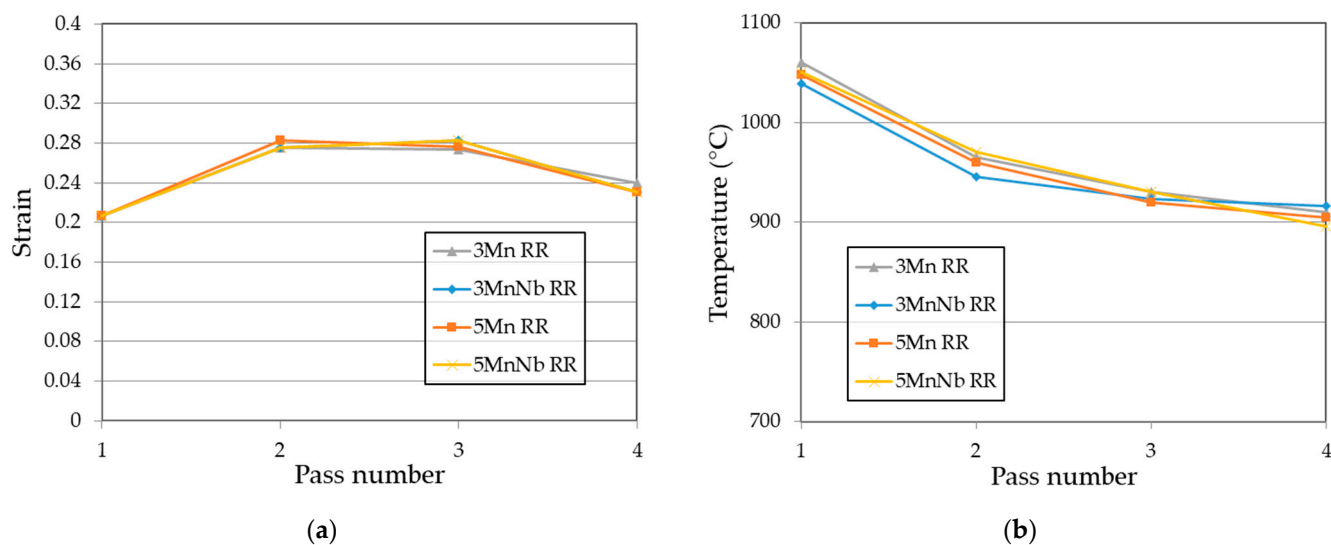


Figure 5. Characteristics of rough rolling: (a) Applied strains; (b) The temperature change; RR—Rough Rolling.

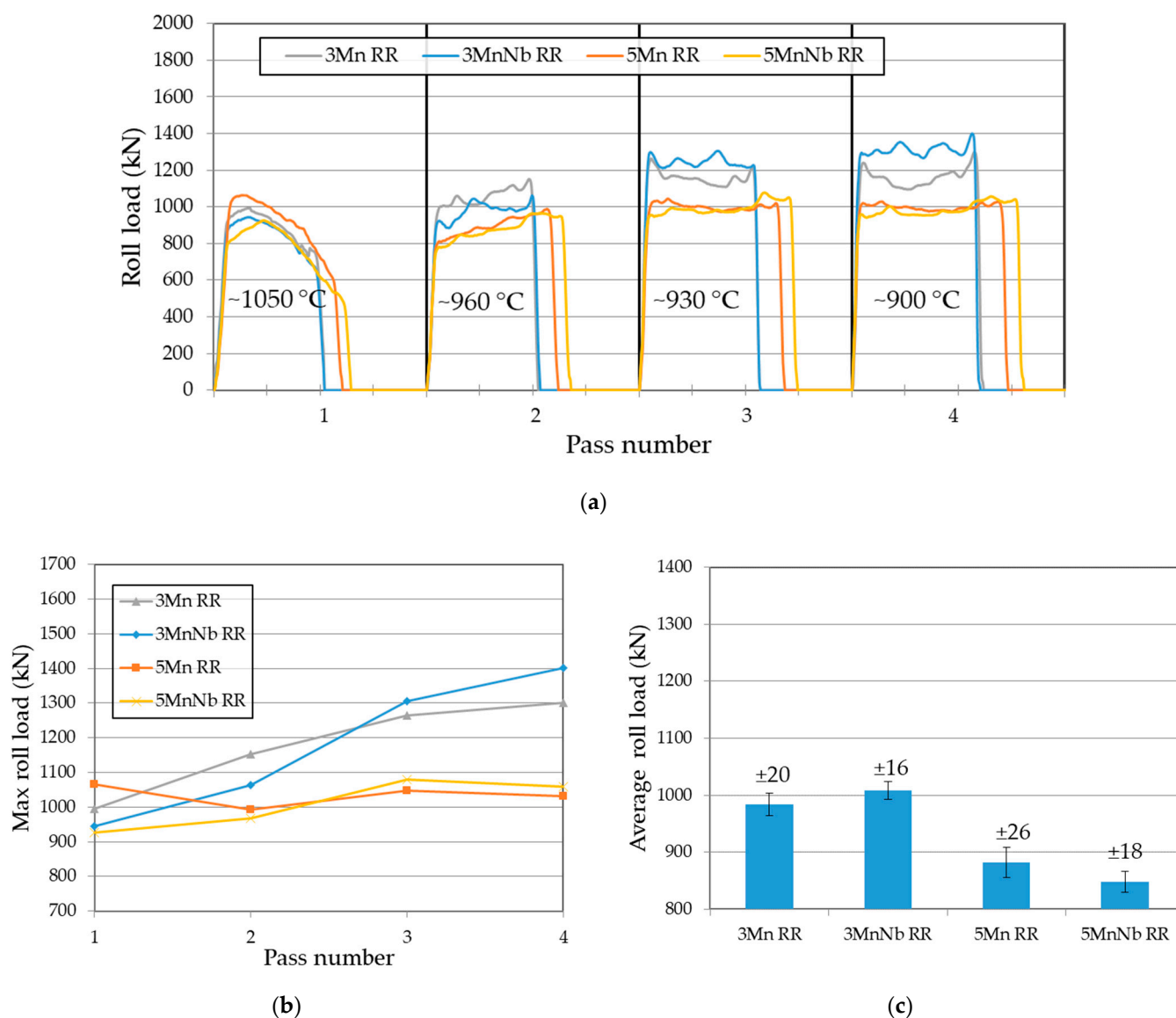


Figure 6. The force parameters of rough rolling: (a) Load-time curves for each steel in subsequent passes; (b) Max load of roll; (c) Average roll load with standard deviation for each steel; RR—Rough Rolling.

The forces for 5Mn and 5MnNb steels are very similar, whereas the 3MnNb steel shows slightly increased loads compared to the Nb-free steel. Figure 6b shows the maximum values of roll loads recorded during each rolling pass. When grouping steels in terms of manganese content, it is visible that, during the first two passes, the steels without Nb addition caused a greater load on the rolls, but in passes three and four, the tendency changed to the opposite. However, the differences are not significant. It is caused by the effect of niobium dissolved in austenite on the delay of the mobility of grain boundaries [30]. The accumulation of deformation and higher strain rates in subsequent passes may initiate the precipitation of carbonitrides in steels with the microaddition of Nb [31,32]. However, the increase in the force for 3MnNb and 5MnNb steels, as compared to the Nb-free steels, is not significant. In the entire range of the deformation temperature, the process controlling the deformation strengthening is dynamic recovery, and the fragmentation of the austenite structure is possible through a partial static recrystallization in the intervals between successive deformations [33]. Figure 6c shows the average values of the roll's load during all four passes. It is clearly visible that both 3Mn and 3MnNb steels generated higher values of force during hot rolling compared to 5Mn and 5MnNb steels.

3.3. Thermomechanical Rolling

The initial dimensions of steels are summarized in Table 3. The force parameters of thermomechanical rolling (Figures 7 and 8) show similar characteristics in relation to the rough rolling results. Applied strain values (Figure 7a) are less consistent due to higher forces required for finishing rolling and the limitations of the used semi-industrial rolling mill. After the first pass, the material shows about 1010–1020 °C (Figure 7b), which is a little bit lower compared to the roughly rolled material of higher initial thickness.

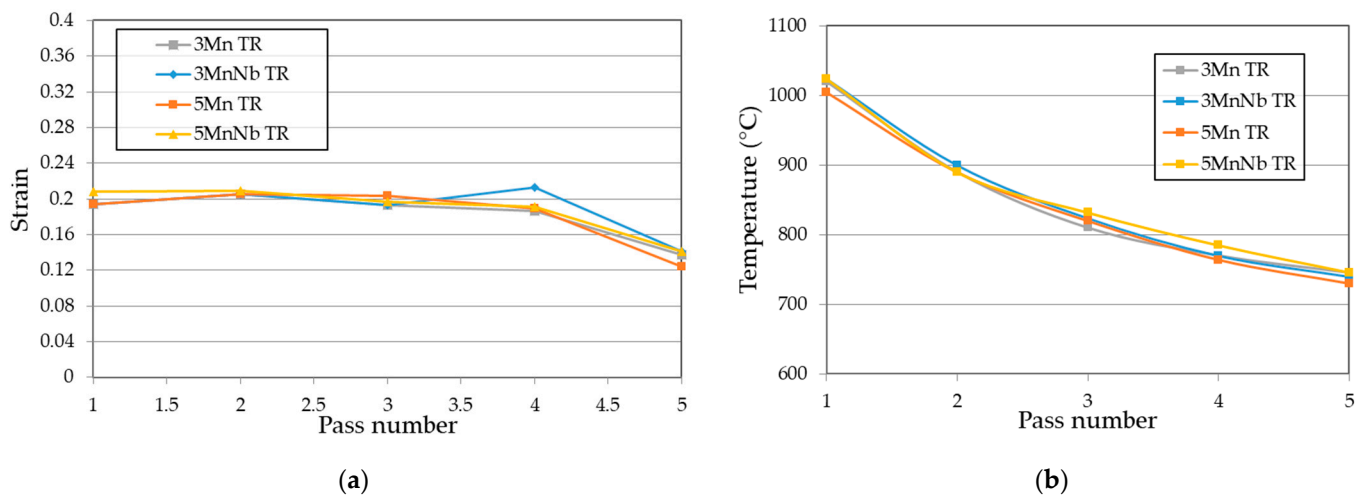


Figure 7. Characteristics of thermomechanical rolling: (a) Applied strains; (b) Temperature change; TR—Thermomechanically rolled samples.

After the fifth pass, sheet samples cooled to about 750 °C, which is in line with the designed value. The roll-load diagram (Figure 8a) also shows that the forces needed to roll alloys containing 3% Mn were higher than those of the 5% Mn steels in this deformation route. Moreover, the forces increased in next passes in the case of all steels (about 400 kN increase from the first to fourth pass). The differences in load are better visible in Figure 8b,c. What is interesting is that previous reports mentioned an increase in hot-rolling resistance with increasing content of alloying additions [34].

In our case, the roll loads are the highest during rolling of steels containing 3Mn and decrease in case of 5Mn steels. This indicates the complex hot-working behavior of medium- and high-Mn steels, which is not linear and changes for some ranges of Mn alloying. In our 3–5% Mn ranges this behavior can be ascribed to faster recrystallization progress with increasing the Mn content from 3 to 5%. This is in line with our earlier results on hot-working behavior investigated in continuous compression tests [30], double-hit compression tests [23] and multi-step simulation of strip rolling [33]. The impact of Nb addition in a range from 0 to 0.04% on the hot-working response is irrelevant for both Mn contents.

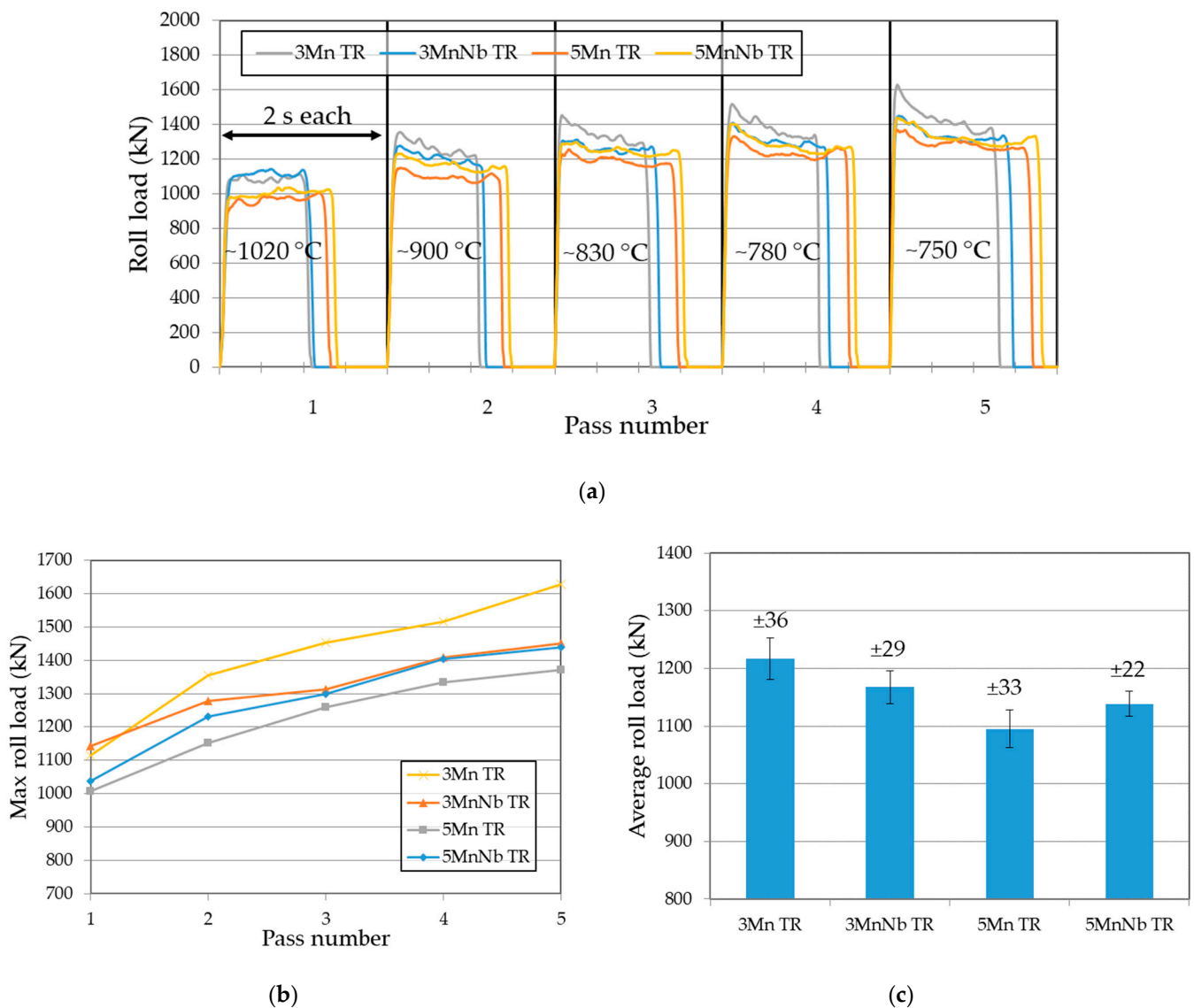


Figure 8. The force parameters of thermomechanical rolling: (a) Load-time curves for each steel in subsequent passes; (b) Max load of roll; (c) Average roll load with standard deviation for each steel; TR—Thermomechanically rolled samples.

After thermomechanical rolling, further grain refinement is visible (Figures 9 and 10) in relation to the forged structures. It concerns both the prior austenite grains and bainitic-martensitic regions. The fraction of RA is also higher, which is related to the deformation-induced carbon enrichment of austenite. This result confirms the impact of the RA size on its stabilization [35]. The fraction of retained austenite is comparable in 3Mn and 3MnNb (Figure 9a,b) steels, but the RA grains are somewhat smaller for the Nb-micro-alloyed steel.

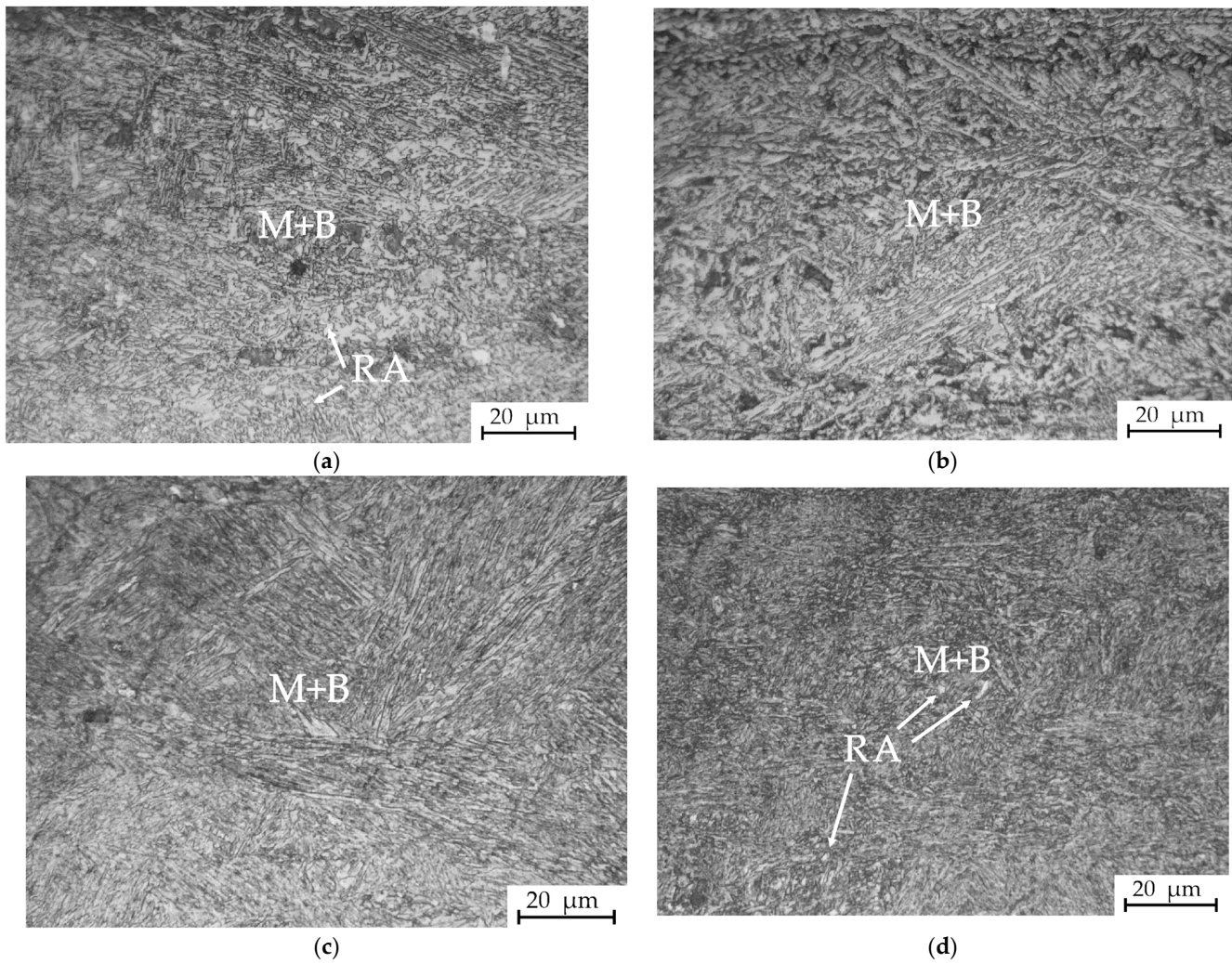


Figure 9. LM images of microstructures after thermomechanical rolling (TR): (a) 3Mn; (b) 3MnNb; (c) 5Mn; (d) 5MnNb; B—Bainite; M—Martensite; RA—Retained austenite.

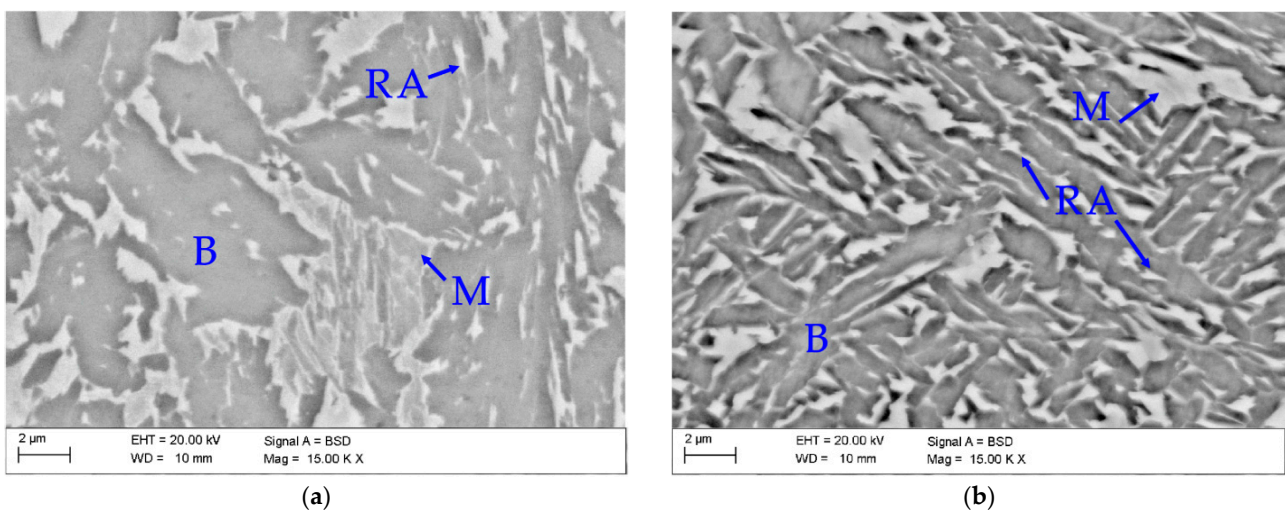


Figure 10. Comparative SEM images of microstructures after forging (a) and thermomechanical rolling (b) of the 3MnNb steel; B—Bainite; M—Martensite; RA—Retained austenite.

Figure 10 presents SEM images of representative 3MnNb steel after successive production stages: forging (Figure 10a) and thermomechanical rolling (Figure 10b). The grain refinement mentioned earlier is clearly visible at this magnification. The forged microstructure contains globular bainite areas and relatively large martensitic blocks (up to $\sim 6 \mu\text{m}$) with retained austenite on their edges. The material after thermomechanical rolling is composed mainly of bainitic laths of smaller thickness ($\sim 1\text{--}1.5 \mu\text{m}$ wide), which are uniformly distributed. The smaller prior austenite grains favor the formation of higher fraction of retained austenite. This is the so-called the mechanical stability effect [36,37].

The fraction of RA in 3Mn steels is higher compared to the 5Mn steels. The differences in RA content ($\sim 15\%$ for steels containing 3% of Mn and $\sim 8\%$ for steels containing 5% of Mn) were confirmed in authors' previous works [38–40], which also provide a wider range of microstructure research and quantitative analysis (XRD, EBSD). It is an interesting phenomenon, since manganese should stabilize austenite. However, the present data are in accordance with the experimental data recently reported by Sugimoto et al. [41]. For the range of steels containing from 1.5 to 5% of Mn the stability of retained austenite depended mostly on the C-enrichment. According to the thermodynamic calculations the carbon content in the austenite decreases with an increase in the Mn concentration. Thus, in the lower-Mn steels, the RA fraction decreases with increasing Mn [30]. This is true for the investigated 3–5 Mn alloying range, which can be treated as lean medium-Mn steels. For the alloys containing above ca. 7% Mn, the austenite is stable despite the lower C-contents in the austenite due to much lower martensite start temperatures, which enable one to stabilize RA at room temperature [42].

4. Conclusions

The paper concerns the semi-industrial process of producing 3–5% medium-Mn steels. The microstructure evolution after casting, forging and thermomechanical rolling was presented. The results provide the force data of four-pass rough rolling and five-pass thermomechanical rolling with direct isothermal holding of the samples in a bainitic region. The results may be useful when implementing the production of MMn steels on an industrial scale. The main conclusions of the study are:

- The applied production process provides obtaining fine-grained multiphase steels with some fractions of retained austenite. For thermomechanically processed steels with a medium-Mn content, the 3Mn concept is more suitable than the 5Mn approach due to the better stabilization of the retained austenite in alloys with the lower Mn content.
- Thermomechanical rolling provides higher microstructure refinement and better homogenization compared to the initial as-forged state.
- The applied semi-industrial rolling line enables the production of good quality sheet samples of medium-Mn steels with a reasonable temperature control and force-energetic parameters acquisition.
- Steels containing 3% Mn generate higher forces both during rough and thermomechanical rolling, which is related to faster recrystallization softening in alloys containing 5% Mn addition.
- The addition of 0.04% Nb has no significant effect on the hot-working behavior of the investigated medium-Mn steels.

Author Contributions: Conceptualization, A.G. and D.W.; methodology, D.W.; validation, A.G., D.W. and A.S.; formal analysis, A.G.; investigation, A.S.; resources, A.G.; data curation, D.W.; writing—original draft preparation, A.S.; writing—review and editing, A.G. and D.W.; visualization, A.S.; supervision, A.G.; project administration, A.G.; All authors have read and agreed to the published version of the manuscript.

Funding: The support of the Faculty of Mechanical Engineering of Silesian University of Technology (Gliwice, Poland) by the statutory funds in 2021 is gratefully acknowledged.

Institutional Review Board Statement: Not applicable.

Informed Consent Statement: Not applicable.

Data Availability Statement: Not applicable.

Acknowledgments: The authors would like to thank the Łukasiewicz Research Network—Institute for Ferrous Metallurgy, Gliwice, Poland for fruitful cooperation in the rolling experiments.

Conflicts of Interest: The authors declare no conflict of interest.

References

1. Kučerová, L.; Opatová, K.; Káňa, J.; Jirková, H. High Versatility of Niobium Alloyed AHSS. *Arch. Metall. Mater.* **2017**, *62*, 1485–1491. [[CrossRef](#)]
2. Kuziak, R.; Kawalla, R.; Waengler, S. Advanced High Strength Steels for Automotive Industry. *Arch. Civ. Mech. Eng.* **2008**, *8*, 103–117. [[CrossRef](#)]
3. Keeler, S.; Kimchi, M.; Mc-oney, P.J. *Advanced High-Strength Steels Application Guidelines V6*; WorldAutoSteel: Middletown, OH, USA, 2017.
4. Grajcar, A.; Radwański, K. Microstructural comparison of the thermomechanically treated and cold deformed Nb-microalloyed TRIP steel. *Mater. Technol.* **2014**, *48*, 679–683.
5. Caballero, F.G.; García-Mateo, C.; Chao, J.; Santofimia, M.J.; Capdevila, C.; de Andrés, C.G. Effects of Morphology and Stability of Retained Austenite on the Ductility of TRIP-Aided Bainitic Steels. *ISIJ Int.* **2008**, *48*, 1256–1262. [[CrossRef](#)]
6. Dobrzański, L.; Borek, W. Structure and Properties of High-Manganese TWIP, TRIP and TRIPLEX Steels. *Aust. J. Multi-Discip. Eng.* **2013**, *9*, 230–238. [[CrossRef](#)]
7. Jabłońska, M.; Niewielski, G.; Kawalla, R. High Manganese TWIP Steel—Technological Plasticity and Selected Properties. *Solid State Phenom.* **2013**, *212*, 87–90. [[CrossRef](#)]
8. Gronostajski, Z.; Niechajowicz, A.; Polak, S. Prospects for the Use of New-Generation Steels of the AHSS Type for Collision Energy Absorbing Components. *Arch. Civ. Mech. Eng.* **2010**, *55*, 221–230.
9. Caballero, F.G.; Chao, J.; Cornide, J.; García-Mateo, C.; Santofimia, M.J.; Capdevila, C. Toughness of Advanced High Strength Bainitic Steels. *Mater. Sci. Forum* **2010**, *638–642*, 118–123. [[CrossRef](#)]
10. Arlazarov, A.; Gouné, M.; Bouaziz, O.; Hazotte, A.; Petitgand, G.; Barges, P. Evolution of Microstructure and Mechanical Properties of Medium Mn Steels during Double Annealing. *Mater. Sci. Eng. A* **2012**, *542*, 31–39. [[CrossRef](#)]
11. Chen, S.; Cao, Z.; Wang, C.; Huang, C.; Ponge, D.; Cao, W. Effect of Volume Fraction and Mechanical Stability of Austenite on Ductility of Medium Mn Steel. *J. Iron Steel Res. Int.* **2019**, *26*, 1209–1218. [[CrossRef](#)]
12. Kozłowska, A.; Janik, A.; Radwański, K.; Grajcar, A. Microstructure Evolution and Mechanical Stability of Retained Austenite in Medium-Mn Steel Deformed at Different Temperatures. *Materials* **2019**, *12*, 3042. [[CrossRef](#)]
13. Ding, R.; Tang, D.; Zhao, A.; Dong, R.; Cheng, J.; Meng, X. Effect of Intercritical Temperature on Quenching and Partitioning Steels Originated from Martensitic Pre-Microstructure. *J. Mater. Res.* **2014**, *29*, 2525–2533. [[CrossRef](#)]
14. Glover, A.; Gibbs, P.J.; Liu, C.; Brown, D.W.; Clausen, B.; Speer, J.G.; De Moor, E. Deformation Behavior of a Double Soaked Medium Manganese Steel with Varied Martensite Strength. *Metals* **2019**, *9*, 761. [[CrossRef](#)]
15. Skowronek, A.; Morawiec, M.; Kozłowska, A.; Pakieła, W. Effect of Hot Deformation on Phase Transformation Kinetics in Isothermally Annealed 3Mn-1.6Al Steel. *Materials* **2020**, *13*, 5817. [[CrossRef](#)] [[PubMed](#)]
16. Adamczyk, M.; Kuc, D.; Hadasik, E. Modelling of Structure Changes in TRIP Type Steel during Hot Deformation. *Arch. Civ. Mech. Eng.* **2008**, *8*, 5–13. [[CrossRef](#)]
17. Kokosza, A.; Pacyna, J. Influence of Austenitising Temperature on Kinetics of Phase Transformations in Medium Carbon TRIP Steel. *Mater. Sci. Technol.* **2015**, *31*, 803–807. [[CrossRef](#)]
18. Paul, S.K. A Critical Review on Hole Expansion Ratio. *Materialia* **2020**, *9*, 100566. [[CrossRef](#)]
19. Hadasik, E.; Kuziak, R.; Kawalla, R.; Adamczyk, M.; Pietrzyk, M. Rheological Model for Simulation of Hot Rolling of New Generation Steel Strips for Automotive Applications. *Steel Res. Int.* **2006**, *77*, 927–933. [[CrossRef](#)]
20. Kučerová, L.; Bystrianský, M. Comparison of Thermo-Mechanical Treatment of C-Mn-Si-Nb and C-Mn-Si-Al-Nb TRIP Steels. *Procedia Eng.* **2017**, *207*, 1856–1861. [[CrossRef](#)]
21. Speer, J.G.; Araujo, A.L.; Matlock, D.K.; de Moor, E. Nb-Microalloying in Next-Generation Flat-Rolled Steels: An Overview. *Mater. Sci. Forum* **2016**, *879*, 1834–1840. [[CrossRef](#)]
22. Ranjan, R.; Beladi, H.; Singh, S.B.; Hodgson, P.D. Thermo-Mechanical Processing of TRIP-Aided Steels. *Metall. Mater. Trans. A* **2015**, *46*, 3232–3247. [[CrossRef](#)]
23. Grajcar, A.; Kuziak, R. Softening Kinetics in Nb-Microalloyed TRIP Steels with Increased Mn Content. *Adv. Mater. Res.* **2011**, *314–316*, 119–122. [[CrossRef](#)]
24. Larrañaga-Otegui, A.; Pereda, B.; Jorge-Badiola, D.; Gutiérrez, I. Austenite Static Recrystallization Kinetics in Microalloyed B Steels. *Metall. Mater. Trans. A* **2016**, *47*, 3150–3164. [[CrossRef](#)]
25. Felker, C.A.; Speer, J.G.; De Moor, E.; Findley, K.O. Hot Strip Mill Processing Simulations on a Ti-Mo Microalloyed Steel Using Hot Torsion Testing. *Metals* **2020**, *10*, 334. [[CrossRef](#)]
26. Nam, A.; Prüfert, U.; Pietrzyk, M.; Kawalla, R.; Prah, U. Simulation of Thermal Phenomena in Reverse Strip-Rolling Process. *Mater. Sci. Forum* **2018**, *941*, 1424–1430. [[CrossRef](#)]

27. Rauch, R.; Bzowski, K.; Kuziak, K.; Uranga, P.; Gutierrez, I.; Isasti, N.; Jacolot, R.; Kitowski, J.; Pietrzyk, M. Computer-Integrated Platform for Automatic, Flexible, and Optimal Multivariable Design of a Hot Strip Rolling Technology Using Advanced Multiphase Steels. *Metals* **2019**, *9*, 737. [[CrossRef](#)]
28. Cabañas, N.; Penning, J.; Akdut, N.; De Cooman, B.C. High-Temperature Deformation Properties of Austenitic Fe-Mn Alloys. *Metall. Mater. Trans. A* **2006**, *37*, 3305–3315. [[CrossRef](#)]
29. Garbarz, B.; Burian, W.; Woźniak, D. Semi-Industrial Simulation of in-Line Thermomechanical Processing and Heat Treatment of Nano-Duplex Bainite-Austenite Steel. *Steel Res. Int.* **2012**, *1*, 1251–1254.
30. Grajcar, A.; Kuziak, R.; Zalecki, W. *Hot Workability of Advanced High Strength Steels with Increased Manganese Content*; METAL: Brono, Czech Republic, 2011; pp. 227–233.
31. Hong, S.G.; Kang, K.B.; Park, C.G. Strain-Induced Precipitation of NbC in Nb and Nb–Ti Microalloyed HSLA Steels. *Scr. Mater.* **2002**, *46*, 163–168. [[CrossRef](#)]
32. Opiela, M.; Grajcar, A. Microstructure and Anisotropy of Plastic Properties of Thermomechanically-Processed HSLA-Type Steel Plates. *Metals* **2018**, *8*, 304. [[CrossRef](#)]
33. Grajcar, A.; Skrzypczyk, P.; Kuziak, R.; Gołombek, K. Effect of Finishing Hot-Working Temperature on Microstructure of Thermomechanically Processed Mn-Al Multiphase Steels. *Steel Res. Int.* **2014**, *85*, 1058–1069. [[CrossRef](#)]
34. Poliak, E.I.; Bhattacharya, D. Aspects of Thermomechanical Processing of 3rd Generation Advanced High Strength Steels. *Mater. Sci. Forum* **2014**, 783–786, 3–8. [[CrossRef](#)]
35. Poddar, D.; Ghosh, C.; Bhattacharya, B.; Singh, V.K. Development of High Ductile Ultra High Strength Structural Steel through Stabilization of Retained Austenite and Stacking Fault. *Mater. Sci. Eng. A* **2019**, 762, 138079. [[CrossRef](#)]
36. Jacques, P.J.; Furnémont, Q.; Lani, F.; Pardoën, T.; Delannay, F. Multiscale Mechanics of TRIP-Assisted Multiphase Steels: I. Characterization and Mechanical Testing. *Acta Mater.* **2007**, *55*, 3681–3693. [[CrossRef](#)]
37. Mukherjee, M.; Mohanty, O.N.; Hashimoto, S.; Hojo, T.; Sugimoto, K. Strain-Induced Transformation Behaviour of Retained Austenite and Tensile Properties of TRIP-Aided Steels with Different Matrix Microstructure. *ISIJ Int.* **2006**, *46*, 316–324. [[CrossRef](#)]
38. Grajcar, A.; Skrzypczyk, P.; Wozniak, D. Thermomechanically Rolled Medium-Mn Steels Containing Retained Austenite. *Arch. Metall. Mater.* **2014**, *59*, 1691–1697. [[CrossRef](#)]
39. Grajcar, A.; Kilarski, A.; Kozłowska, A. Microstructure–Property Relationships in Thermomechanically Processed Medium-Mn Steels with High al Content. *Metals* **2018**, *8*, 929. [[CrossRef](#)]
40. Grajcar, A.; Kilarski, A.; Kozłowska, A.; Radwański, K. Microstructure Evolution and Mechanical Stability of Retained Austenite in Thermomechanically Processed Medium-Mn Steel. *Materials* **2019**, *12*, 501. [[CrossRef](#)]
41. Sugimoto, K.; Tanino, H.; Kobayashi, J. Impact Toughness of Medium-Mn Transformation-Induced Plasticity-Aided Steels. *Steel Res. Int.* **2015**, *86*, 1151–1160. [[CrossRef](#)]
42. Soleimani, M.; Kalhor, A.; Mirzadeh, H. Transformation-Induced Plasticity (TRIP) in Advanced Steels: A Review. *Mater. Sci. Eng. A* **2020**, 795, 140023. [[CrossRef](#)]